



Contents lists available at ScienceDirect



Catalysis Today

journal homepage: www.elsevier.com/locate/cattod

Direct Au-Ni/Al₂O₃ catalysed cross-condensation of ethanol with isopropanol into pentanol-2

A.V. Chistyakov^{a,b,*}, P.A. Zharova^a, S.A. Nikolaev^c, M.V. Tsodikov^{a,b}

^a Topchiev Institute of Petrochemical Synthesis RAS, Leninskii pr. 29, Moscow 119991, Russia

^b Semenov Institute of Chemical Physics RAS, Kosygin str., 4, Moscow 119991, Russia

^c Moscow State University, Leninskie Gory 1, Moscow 119991, Russia

ARTICLE INFO

Article history:

Received 30 December 2015

Received in revised form 6 June 2016

Accepted 7 June 2016

Available online xxx

Keywords:

Cross-condensation

Au-Ni synergism

β-alkylation

Ethanol

Isopropanol

Guerbet reaction

ABSTRACT

Ethanol and isopropanol cross-condensation 0.2Au-0.06Ni/γ-Al₂O₃ catalyst have been developed based on the synergistic effect of gold and nickel in many reactions. A cross-condensation reaction results in the formation of pentanol-2 and pentanone-2 in high yields in the absence of any alkali or sacrificial agents (e.g., hydrogen acceptors or hydrogen donors). In this study, heterogeneous Au-Ni/Al₂O₃ catalysts were used in this type of reaction for the first time. The catalyst developed in this study is also effective for the self-condensation of ethanol, providing 85% selectivity of linear α-alcohols at 63.5% ethanol conversion. Structural investigations show that the morphological peculiarities and charge state of gold may produce the different activities of mono- and bimetallic Au- and Ni-containing catalysts.

© 2016 Elsevier B.V. All rights reserved.

1. Introduction

Alcohols are an important class of organic compounds due to their wide variety of uses in industrial and laboratory chemistry. Due to the increasing availability of bio-based alcohol feedstocks, we propose a chemical route to convert fermentation products (e.g., ethanol and isopropanol) into pentanol-2 in this study. Ethanol can be produced via the fermentation of sugar-containing or lignocellulose feedstock [1]. Isopropanol may be efficiently produced from lignocellulosic biomass via cellobiose degradation [2] or the isopropanol–butanol–ethanol (IBE) process [3].

The synthesis of higher alcohols from lower alcohols is generally known as the Guerbet reaction, in which basic catalysts are typically used [4,5]. The Guerbet reaction is an important method when constructing complex molecules from simple substrates and has thus attracted marked interest in recent years [6]. Both alcohol self-condensation and cross-condensation includes four general reaction steps: the alcohol is first dehydrogenated, after which the carbonyl compounds are coupled via aldol addition and subsequent dehydration; finally, the compounds are hydrogenated into saturated alcohols [5]. Depending on the types of alcohols used in the

reaction (e.g., primary versus secondary, long chain versus short chain), branched or unbranched products can be formed. Additionally, when different alcohols are present in the reaction, both self-coupling and cross-coupling reactions can occur [7].

Many examples of alcohol self-condensation can be found in the literature that can be categorized into three primary catalytic composition types: (1) homogeneous base combined with homogeneous transition metals; (2) homogeneous base combined with heterogeneous transition metals; and (3) heterogeneous systems with or without transition metals [7]. The use of alkali compounds creates certain implications for use in industry, such as the stability of the dehydrogenation catalyst, reactor vessel corrosion and intensive product purification. The application of heterogeneous catalytic systems provides easy separation from the reaction mixture, does not cause corrosion and metal leaching, and can ideally be reused multiple times without extensive regeneration. To develop cost efficient Guerbet processes, the use of solid acid-base catalysts is required.

The conversion of ethanol into *n*-butanol over purely heterogeneous catalysts has been reported in several publications and patents [8–18]. Generally, the reaction temperature varies from 200 up to 450 °C with a relatively low conversion (e.g., 10%–20%) and a selectivity approaching 70%. Hydroxyapatites have been shown to be the most active and selective catalytic systems for higher alcohols production [10,11]. In a plug flow reactor, the highest *n*-

* Corresponding author at: Laboratory of Catalytic Nanotechnologies, Topchiev Institute of Petrochemical Synthesis RAS, Leninskii pr. 29, Moscow 119991, Russia.

E-mail address: chistyakov@ips.ac.ru (A.V. Chistyakov).

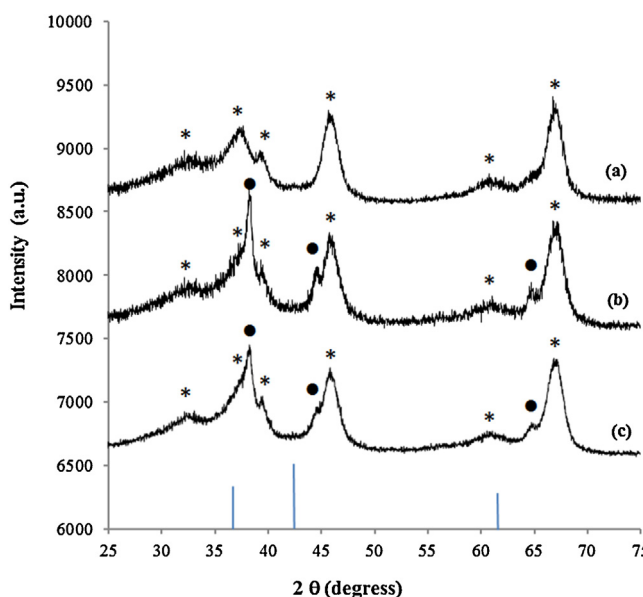


Fig. 1. XRD pattern of catalysts: (a) Ni/Al₂O₃, (b) Au/Al₂O₃ and (c) Au-Ni/Al₂O₃. The symbol (*) indicates reflections of gamma alumina (JCPDS card, No. 29-0063). The symbol (●) indicates reflections of gold crystallites (JCPDS card, No. 04-0784). The vertical lines indicated the position of the most intense reflections of nickel oxide (JCPDS card, No. 78-0643).

butanol selectivity was found to be 76.3% at 14.7% conversion of ethanol [11] and 81.2% at 7.6% conversion of ethanol [10]. The study of a batch reactor process showed that a 20% Ni/Al₂O₃ catalyst manufactured by Crossfield produces the highest selectivity of 80% at a conversion of approximately 25% after 72 h [12].

Isopropanol condensation generally leads to ketones formation due to its higher rate of acetone alkylation compared to Guerbet condensation. Over hydrotalcite-derived mixed oxide (Mg₃AlO_x), the primary products are diacetone alcohol, phorone and isophorone [19]. The Guerbet reaction of supercritical isopropanol into a small amount of 3,3,5-trimethylcyclohexanol was observed in a study of the decomposition of epoxy resin with KOH [20]. The self-coupling of 2-propanol occurred with a heterogeneous Ni/CeO₂ catalyst [21] (>200 °C) and various coupling products, including methyl isobutyl ketone (21%), 4-methyl-2-pentanol (19%), diisobutyl ketone (21%) and 2,6-dimethyl-4-hexanol (9%), were obtained in comparable yields to previous studies [22–24].

Several examples are shown to describe acetone-butanol-ethanol (ABE) fermentation products conversion in comparison to Guerbet type catalysts [25,26]. In both catalytic systems studied in these works, the formation of ketones C₇–C₁₉ was observed, which indicates that no interaction between the ethanol and acetone occurred. The formation of 2-pentanone occurred only in the presence of Pd-hydrotalcite catalyst, and its yield did not exceed 10% from other C₇–C₁₁ ketones [26]. The fermentation mixture of the IBE conversion also did not lead to C₅ product formation. The condensation of secondary alcohols with primary alcohols thus effectively catalysed by homogeneous base and homogeneous/heterogeneous transition metal systems [9,27,28] but never a pure heterogeneous catalytic system.

Gold had long been considered to be a catalytically inert metal until Haruta et al. found the surprisingly high activity of gold nanoparticles during low-temperature CO oxidation [29]. The recent progress in heterogeneous catalysis resulted in remarkable investigations that showed the high catalytic activity of gold nanocomposites in the water-gas shift reaction [30,31], hydrogenation [32,33], isomerization [34,35], hydrodechlorination [36,37]

and other reactions [38]. It was reported in references [39,40] that the modification of gold with a small amount of transition metals might result in synergistic interactions between the Au and M phases that markedly enhance the catalytic performance of poly-metallic Au-M catalysts. Although it is generally accepted that the high activity of monometallic Au catalysts can be attributed to the presence of small gold crystallites (i.e., <4 nm) [41], the nature of the most active sites in poly-metallic gold-contained catalysts remains under discussion. Certain authors report that ionic gold is formed on the surface of Au-M catalysts and provides a high synergistic activity [42,43], while others claim that metallic nano-sized gold contains the most active sites [44]. Additionally, a third group of authors reports that the rough shape of particles [45], the atoms on the interface between gold and the second metal [41], the specific surface chemistry of bimetallic alloys [38,39] are most important for synergistic activity.

Gold-nickel catalysts possess high synergistic activities and long lifetimes when converting a variety of hydrocarbons, such as *n*-butane [46], allylbenzene [47], ethyne [48], and dichlorophenols [49]. The results of these studies and other recent findings [50] on the γ-Al₂O₃ supported Au-Ni catalysed ethanol conversion into hydrocarbons C₃–C₉ indicate that gold-nickel nanocomposites are promising for the cross-condensation of ethanol with isopropanol into other valuable chemicals.

This study compares the direct cross-condensation of ethanol with isopropanol in the presence of synergistic Au-Ni/Al₂O₃ catalyst and its monometallic analogues (Au/Al₂O₃ and Ni/Al₂O₃). This study is the first to investigate the catalytic performance of Au-Ni catalysts in this reaction. To describe the differences between the structure of supported metals in catalysts, X-ray diffraction (XRD) analysis, energy dispersive X-ray (EDX) analysis and transmission electron microscopy (TEM) were performed. Structural investigations of Au-Ni/Al₂O₃, Au/Al₂O₃ and Ni/Al₂O₃ catalysts were conducted via X-ray photoelectron spectroscopy (XPS), infrared spectroscopy (IR) of adsorbed CO; X-ray absorption spectroscopy (XAS) was also performed and published earlier in reference [47]. The relationships between a compound's structure, activity and mechanistic aspects are discussed to clarify the factors that may affect the synergistic effect in the presence of the Au-Ni catalyst.

2. Experimental

2.1. Catalysts preparation

Gamma alumina (Catalyst LLC, grains $\phi = 0.5$ mm, $S = 160 \text{ m}^2/\text{g}$) was used as a support for the catalysts. Aqueous solutions of Ni(NO₃)₂ and HAuCl₄ (Sigma-Aldrich, 98–99% pure) were used as metal precursors.

Ni/Al₂O₃ (Ni = 0.06 wt.%) catalyst was produced via impregnation, as described in reference [47]. Al₂O₃ (5 g, calcined at 400 °C for 3 h) was first impregnated with 5.5 mL of an aqueous solution containing the desired amount of nickel. Then, the wet solid was dried at 24 °C for 24 h and calcined at 400 °C for 6 h.

Monometallic Au/Al₂O₃ (Au = 0.2 wt.%) catalysts with a metal content similar to Ni/Al₂O₃ was produced via deposition-precipitation, as described in references [47,51]. An aqueous solution of HAuCl₄ with the desired concentration of gold was adjusted to pH = 7.0 by adding NaOH (0.1 M). Then, Al₂O₃ (10 g, calcined at 400 °C for 3 h) was dispersed in this solution while being stirred at 50 °C for 1 h. The solid was washed with water to remove Cl⁻, dried at 24 °C for 24 h, and calcined at 400 °C for 3 h. The obtained precursor was then separated into two parts: the first part (5 g) was calcined at 400 °C for 3 h to fabricate Au/Al₂O₃ (Au = 0.2 wt.%); the second part (5 g) was impregnated with an

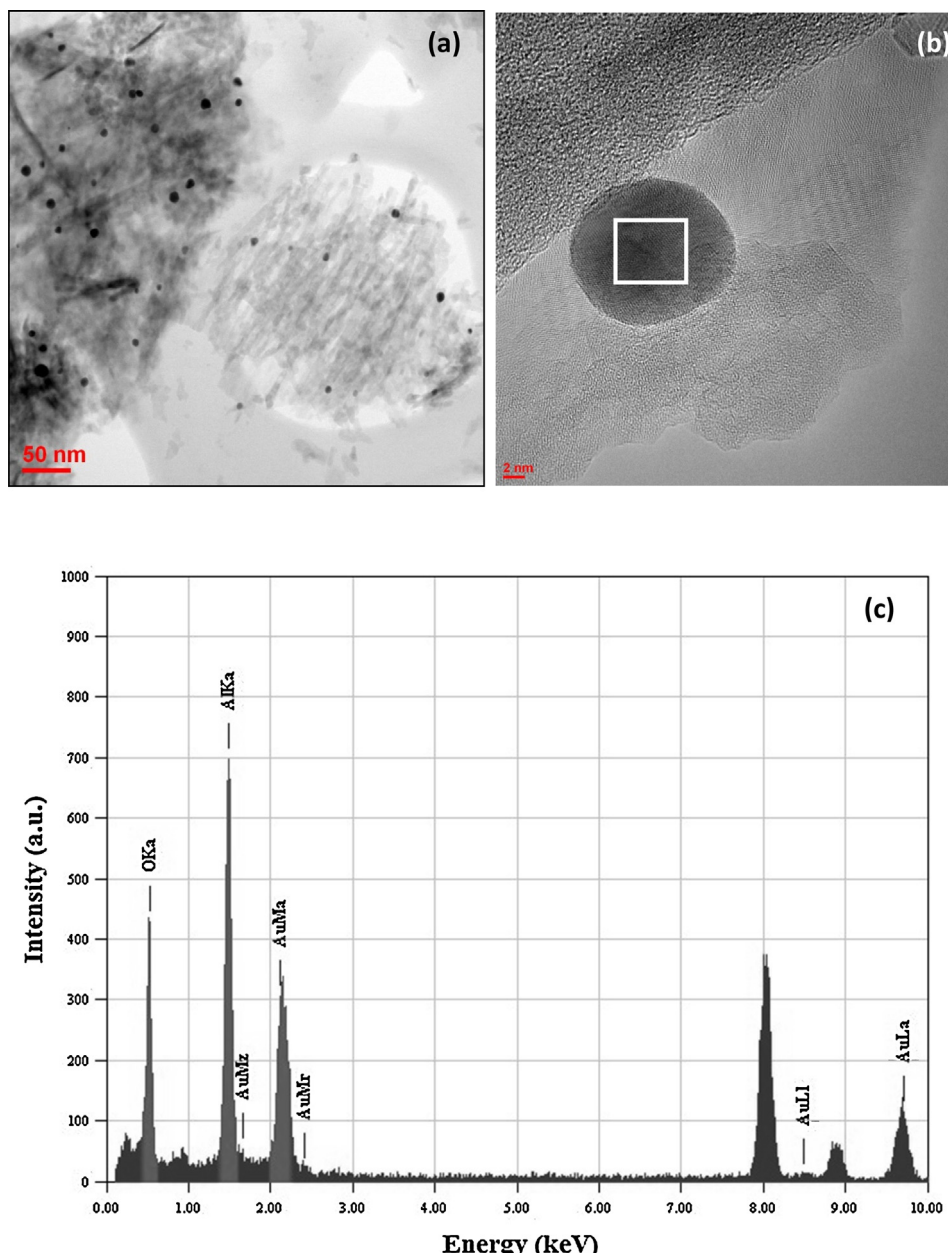


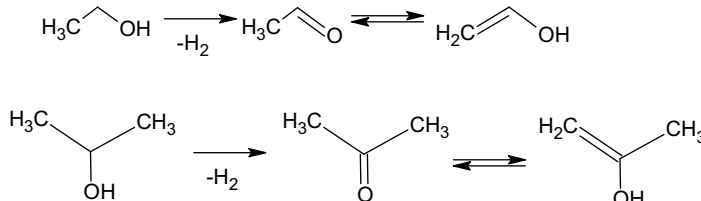
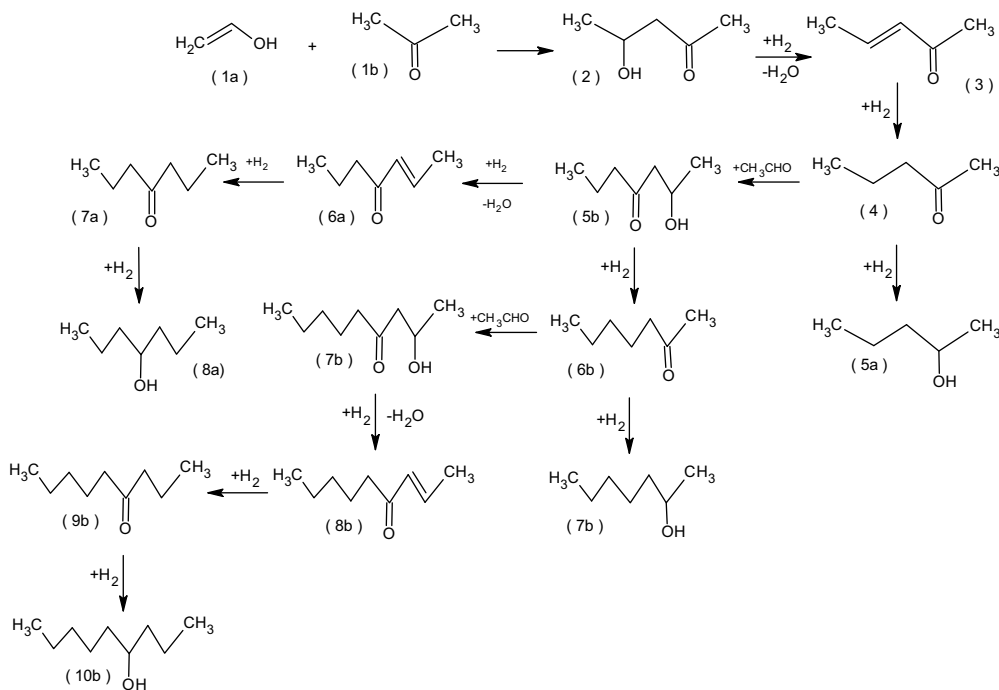
Fig. 2. Morphological features Au/Al₂O₃ catalyst: (a) TEM image of the surface; (b) HRTEM image of a dark spherical structure; and (c) EDX spectrum of the square selected on the HRTEM image.

aqueous solutions of Ni(NO₃)₂, dried, and calcined at 400 °C for 3 h to create Au-Ni/Al₂O₃ (Au = 0.2 wt.%; Ni = 0.06 wt.%).

The real metal content in the catalysts was determined using atomic absorption spectroscopy (AAS) on a Thermo iCE 3000 AA spectrometer. A catalyst (0.1 g) was treated with 10 mL of aqua regia (HCl:HNO₃ = 4:1) for 1 h. This mixture was added to 90 mL of H₂O. The metal content in the solution were measured by AAS with application of the calibration curves [52]. The relative error in the determination of the metal concentration in solutions was $\pm 1\%$. The real metal content in the catalyst [C₁] was calculated as [C₁] = [C₂] × 100 mL × 0.1 g⁻¹ × 100%, where [C₂] is the metal content in the 100-mL solution measured by AAS. The real metal content in the catalysts was 0.2 wt.% (Au) and 0.06 wt.% (Ni), which correspond to the desired metal content.

2.2. Catalyst characterization

XRD analysis was performed on a Bruker D8 Advance diffractometer with Ni-filtered Cu K α radiation and a LYNXEYE detector. Specimens were prepared via mechanical dispersion of the catalysts. Diffraction data were collected in the 2 θ range from 20 to 80° and with a step size of 0.02°. TEM analysis was performed on a JEOL JEM 2100F/UHR microscope with a 0.1-nm resolution. Specimens were prepared via ultrasonic dispersion of the catalysts (0.2 g) in ethanol (10 mL) followed by the deposition of a drop of suspension on a Cu grid coated with carbon. Dark spots in the TEM images indicated the presence of metal particles, and the determination of the composition of metal particles was performed using EDX analysis using a JED-2300 X-ray spectrometer. The size of individual particle was calculated as a maximum linear size. For each catalyst, 300–380 particles were processed to determine the particles' size distribution and the mean particle size.

Substrate activation*Reaction route***Scheme 1.** Schematic presentation of the cross-condensation of ethanol with isopropanol.**2.3. Catalytic reaction**

Analytical-grade ethanol and isopropanol were used without further purification. Catalytic experiments were performed in a 45-mL high-pressure Parr autoclave equipped with magnetic stirring. The reactor was loaded with the catalyst (typically 4.5 g). The catalyst testing procedure occurred as follows: (1) the reactor with the catalyst was loaded with equal volumes of ethanol and isopropanol (typically 15 mL each) or with 30 mL of ethanol or isopropanol for self-condensation tests; (2) the reactor was closed and flushed with inert gas (Ar); (3) the reactor was heated at a heating rate of 20 °C/min; (4) the reaction was allowed to occur for 5 h; (5) the reactor was cooled down; and (6) the reaction mixture was analysed.

Qualitative and quantitative analyses of the C₁–C₅ hydrocarbon gases were performed via gas chromatography (GC) with a Kristall-4000 M chromatograph (carrier gas: He, column: HP-PLOT/Al₂O₃, 50 m × 0.32 mm; flame ionization detector). GC analyses of CO, CO₂ and H₂ were performed with a Kristall-4000 chromatograph (carrier gas: Ar, column: SKT, 1.5 m × 4 mm; thermal conductivity detector). The qualitative composition of the liquid organic products was performed via gas-liquid chromatography coupled to a mass spectrometry (GLC-MS) using MSD 6973 and Autowt.-150 spectrometers (EI = 70 eV, columns: HP-5MS, 50 m × 0.32 mm and CPSil-5, 25 m × 0.15 mm). The quantitative content of the organic

Table 1
Conversion of ethanol and isopropanol (T = 275 °C; P = 150 atm^a, 5 h).

Catalyst	Au-Ni/Al ₂ O ₃		Au/Al ₂ O ₃		Ni/Al ₂ O ₃	
	EtOH	i-PrOH	EtOH	i-PrOH	EtOH	i-PrOH
Substrate	63.5	35.1	30	27.4	5.8	7.5
Selectivity (%)						
Butanol-1	58.4	0	15.9	0	0.3	0
Hexanol-1	21.2	0	0.5	0	0	0
Octanol-1	5.6	0	0	0	0	0
Propane	0	15.3	0	17.9	0	2.3
Acetone	0	81.5	0	76.4	0	61.5
Others	14.8	3.2	83.6	5.7	99.7	36.2

^a Initial pressure of reagent.

compounds present in a sample was determined via GLC using a Varian 3600 chromatograph (carrier gas: He, column: Chromtec SE-30, 25 m × 0.25 mm detector: flame ionization detector).

3. Results and discussion

First, we tested the activity of the 0.2Au-0.06Ni, 0.2Au and 0.06Ni catalysts for the self-condensation of ethanol and isopropanol (Table 1). The bimetallic 0.2Au-0.06Ni catalyst showed the highest yield of condensation products, such as butanol-1, hexanol-1 and octanol-1 with a total selectivity of 85.2% at 63.5%

Table 2

Substrates conversion and cross-condensation products selectivity depending on catalyst composition (275 °C, 5 h).

Catalyst	Au-Ni/Al ₂ O ₃ ¹	Au-Ni/Al ₂ O ₃	Au/Al ₂ O ₃
Selectivity of alkylation product (%)	66.1	66.9	33.8
Ethanol conversion (%)	39.3	38.2	46.7
i-propanol conversion (%)	37.2	42.3	56.4
Product N in Scheme 1	Selectivity (%)		
pentanone-2	4	14.2	15.1
pentanol-2	5a	35.7	37.2
heptanone-4	7a	3.1	3.4
heptanone-2	6b	1.1	1.9
heptanol-4	8a	7.0	7.2
heptanol-2	7b	0.8	0.9
nonanone-4	9b	0.4	0.5
nonanol-4	10b	0.5	0.7

¹ Data obtained after ten successive experiments (5 h each).

conversion of ethanol. Conversely, the 0.06Ni system primarily catalysed the dehydration of ethanol to provide diethyl ether and ethylene, and dehydrogenation to provide acetic aldehyde. The conversion and selectivity to linear alcohols in the presence of Ni catalyst does not exceed 5.8 and 0.3%, respectively. An Au analogue was then used to catalyse the conversion of ethanol primarily into butanol-1 but produced a low conversion (30%) and low selectivity (16.4%).

The results obtained in this study show the highest ratio of linear α -alcohols selectivity and ethanol conversion. The best known analogues show that only 10%–15% of supercritical ethanol converts at a 50%–60% selectivity of butanol-1 after 5 h in batch mode with catalyst containing more than 20% Ni/Al₂O₃. The maximum ethanol conversion (25%) was observed only after 72 h, which produced a selectivity of approximately 80% [14]. In plug-flow mode, the highest selectivity of 1-butanol ever reported was 83–87% at an ethanol conversion of 7%–9%. However, during ethanol conversions up to 40%, a decrease was observed down to a selectivity of 60%. Neither hexanol-1 nor octanol-1 were found in the resulting product mixture [10]. The highest productivity in a plug-flow mode was reported by Takahasi et al. [11]. The selectivity of alcohols C₄–C₁₀ achieved 86.1% at an ethanol conversion of 14.7%. A comparable ethanol conversion (57.4%) was achieved at alcohols C₄–C₁₀ selectivity of as low as 63.6%, which is similar to that shown in this study (63.5%).

Next, the scope of isopropanol for self-condensation using 0.2Au-0.06Ni, 0.2Au and 0.06Ni catalysts was investigated. The results of this study show that isopropanol undergoes no self-condensation. The primary products were acetone and propane over 0.2Au-0.06Ni and 0.2Au catalysts (Table 1). The 0.06Ni system catalysed the isopropanol dehydrogenation into acetone and dehydration into propene, as shown in Table 1. Alumina based systems typically catalyse the dehydrogenation of secondary alcohols to provide corresponding ketones as primary products [8].

The cross-condensation of ethanol with isopropanol into alcohols and ketones (C₅, C₇, C₉) was found to occur in the presence of bimetallic Au-Ni/Al₂O₃ and monometallic Au/Al₂O₃ catalysts (Table 2). The monometallic Ni/Al₂O₃ catalyst showed no activity in this process. Probable pathways of cross-condensation of ethanol with isopropanol are shown in Scheme 1. Feeding alcohol conversions that are approximately equal may indicate the equable filling of the active surface with chemisorbed substrates and its equable activity. The total selectivity of cross-condensation products is shown to be 66%; the primary by-products are diethyl ether (S=4%), butanol-1 (S=10%) and acetone (S=10.6%). Thus ethanol takes part in two parallel reactions: cross-condensation with isopropanol; and self-aldehydization, leading to butanol-1 formation. In the reaction products, only traces of acetic aldehyde were found, indicating the equable activity of the substrates with

regard to dehydrogenation with the formation of acetic aldehyde and acetone (see Scheme 1, Substrate activation). Acetic aldehyde and acetone exhibit markedly different activities: acetic aldehyde rapidly converts into butanol-1 or interacts with isopropanol with pentanol-2 formation, while acetone is less active and has a tendency to accumulate in the reaction products.

The primary product of the interaction of ethanol and isopropanol is pentanol-2, whose selectivity reaches 35%–37%. The selectivity of pentanone-2 is 14%–15%, which indicates the low efficiency of steps 4 and 5a shown in Scheme 1. However, in the reaction products, there are no unsaturated alcohols or ketones (3, 6a, 8b). Thus, the Au-Ni/Al₂O₃ catalyst shows the highest efficiency during the dehydrogenation and hydrogenation of unsaturated C=C bonds steps. Based on Scheme 1 and Table 2, pentanol-2 during interaction with acetic aldehyde primarily converts into heptanone-4, followed by hydrogenation into heptanol-4. The primary by-product of this step (4 → 8a) is heptanone-2, which undergoes hydrogenation into heptanol-2 (6b → 7b) or interacts with acetic aldehyde molecule forming nonanone-4 and/or nonanol-4. Alcohols containing more than nine carbon atoms in its carbon skeleton were not observed among reaction products.

The cross-condensation process was performed under rather sever conditions (275 °C, 150 atm, 5 h, batch mode). The supported metals in the catalysts could interact with the alcohols and/or be washed away from the surface of the catalysts via organic media under these conditions. This process results in a decrease in the concentration of active components and the deactivation of catalyst. To verify this hypothesis, ten 5-h consecutive experiments were performed. The results of the tenth experiment are shown in Table 2. The conversion and cross-condensation products' selectivity are shown to be similar to those observed with the initial catalyst after one 5-h experiment. Additionally, the concentration of Au and Ni after 50 h corresponds to the initial concentration of nickel and gold when considering the uncertainty of the instrumentation used in this study. The most probable reason for the high stability of the Au-Ni catalyst is the strong interaction between the supported metals, which decreases their mobility.

3.1. Structural peculiarities of mono and bimetallic systems

The XRD patterns of Au, Ni and Au-Ni catalysts are shown in Fig. 1. Six diffraction peaks at 2θ equal to 32.4, 37.5, 39.5, 46.0, 61.1, and 66.8° are shown on each diffraction pattern. These peaks are assignable to the (220), (311), (222), (400), (511), and (440) planes of γ-Al₂O₃ (JCPDS card, No. 29-0063). The patterns of the Au and Au-Ni catalysts possess peaks at 2θ equal to 38.1, 44.4 and 64.6°. These peaks are attributable to gold crystallites (JCPDS card, No. 04-0784). Unfortunately, no peaks of any Ni species were found with the Ni and Au-Ni catalysts in this study. The absence of diffraction peaks in the XRD patterns of nanocomposites is a rather typical situation and could be explained by the high dispersion and/or relatively low metal content of the catalysts.

A previous investigation of the Au, Ni and Au-Ni catalysts showed that nickel in both Au-Ni/Al₂O₃ and Ni/Al₂O₃ catalysts exist as Ni²⁺ cations; gold in the Au/Al₂O₃ catalyst exists as Au⁰; and Au⁰ nanoclusters co-exist with Auⁿ⁺ ($1 \leq n \leq 3$) cations in the bimetallic Au-Ni/Al₂O₃ catalyst [47]. Those results were found using XPS, DRIFT, and XAS techniques.

Dark spherical spots are visible in the TEM and HRTEM images of the Au catalyst (Fig. 2(a), (b)). The EDS spectrum of these spots exhibits peaks corresponding to C, Cu, Al, O and Au elements (Fig. 2(c)). The presence of Cu and C elements can be attributed to the TEM grid and should not be considered. The remaining combination of elements indicates that the dark spots visible in the TEM images can be attributable to gold particles deposited onto the alumina surface (Fig. 3(b)). The size of the detected gold particles

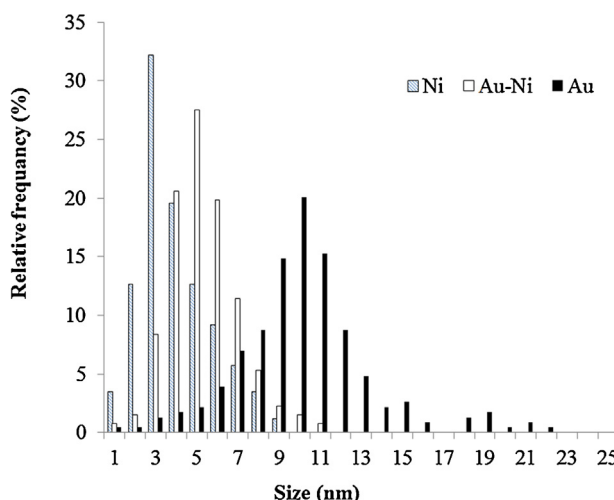


Fig. 3. Particles size distributions for the Au/Al₂O₃, Ni/Al₂O₃ and Au-Ni/Al₂O₃ catalysts.

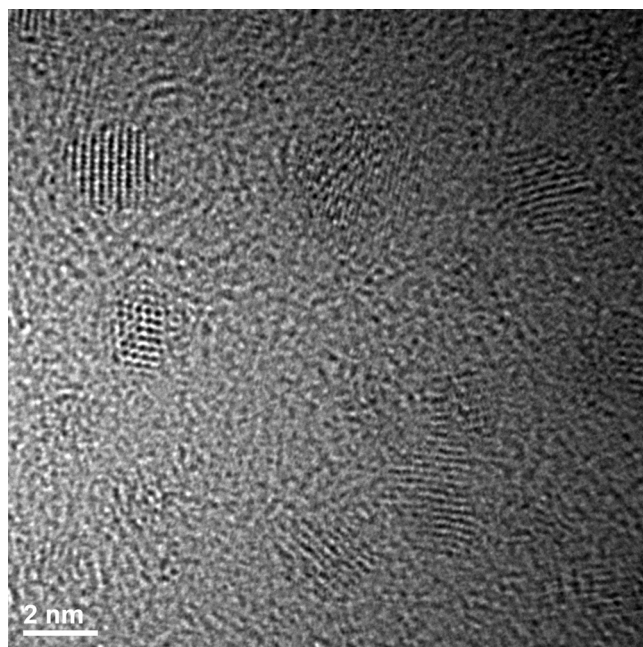


Fig. 4. HRTEM image of nickel particles in the Ni/Al₂O₃ catalyst.

in the Au catalyst is between 1 and 23 nm, and the average size is 10 ± 2 nm (Fig. 3). The HRTEM image of individual nickel particles in the Ni/Al₂O₃ catalyst is shown in Fig. 4 and illustrates the rounded shape of supported particles. The size of the detected nickel particles in Ni catalyst is between 1 and 9 nm, and the average size is 3 ± 0.5 nm (Fig. 3).

The particles size distribution of the Au-Ni catalyst shows the absence of particles with a size of >15 nm. The average size of the particles in the Au-Ni catalyst is shifted to smaller clusters by 5 nm. These features indicate that Au-Ni interaction prevents the mobility of supported metals, which are primarily gold nanoparticles. The results of this study agree with the TEM studies of Au-M supported catalysts [38,39,53]. Another interesting feature of the Au-Ni catalyst is the formation of relatively large clusters, as shown in Fig. 5. The TEM-EDX analysis shows that these clusters consist of individual Au and Ni particles that are in close contact with each other (Figs. 6 and 7). Investigating 230 particles that are situated both inside and outside of these clusters shows that the relative con-

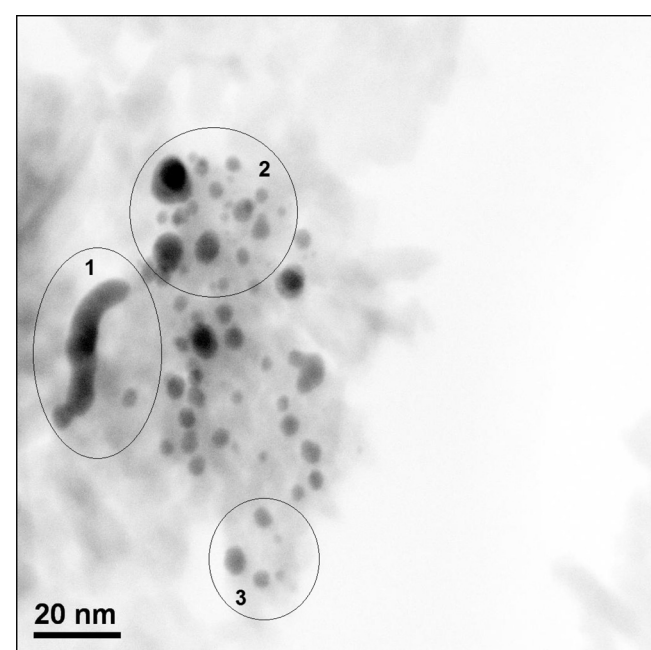


Fig. 5. TEM images of the supported nanoparticles in the Au-Ni/Al₂O₃ catalyst.

tent of gold particles situated in close contact (i.e., within <1 nm) of nickel particles is 80%; the remaining 20% are either gold or nickel particles that located far from each other (i.e., the distance to the nearest particle is >10 nm).

3.2. Probable reasons of the different catalytic activities of mono and bimetallic systems

The higher selectivity of condensation-product formation at relatively equal ethanol and isopropanol conversions of bimetallic Au-Ni/Al₂O₃ catalyst compared to monometallic Au/Al₂O₃ may be caused by the following phenomena. The first phenomenon is the interaction of Au and NiO species, which produces an increase in the dispersion of gold clusters from 10 to 5 nm. Thus, with equal gold content, the Au-Ni/Al₂O₃ catalyst should have a larger gold surface area. Fig. 4 shows that in the bimetallic system, elongated clusters of Au_n-NiO_{xn}-Au_n-NiO_{xn} are formed. Such clusters are favourable to the multiple coordination of ethanol and isopropanol molecules and, consequently, facilitate the growth of alcohols' hydrocarbon skeletons.

The second phenomenon could be linked to the formation of gold cations Auⁿ⁺, where $1 \leq n \leq 3$. Scheme 1 shows that alkylation product formation passes through the dehydrogenation-hydrogenation steps. Typically, these processes for metal-containing catalysts are accompanied by a change in oxidation state from M⁰ to M⁺². For the monometallic catalyst Au/Al₂O₃, this change may be described by the equation Au⁰ → Au⁺² → Au⁰, which includes an uncharacteristic oxidation state of +2 for gold. This reaction may explain the low selectivity of Au clusters in the Au/Al₂O₃ catalyst. In the bimetallic system, gold is primarily present as cations with charge state near +1, which allows for the activation of hydrogenation-dehydrogenation cycle with common charge states of gold: Au⁺¹ → Au⁺³ → Au⁺¹. Thus, one-pot β-alkylation of isopropanol with ethanol is more effective over bimetallic system. However, as shown in Table 2, the ratio of alcohol/ketone formation selectivity is approximately 2/1, indicates that the hydrogenation activity of Au-Ni/Al₂O₃ catalyst is insufficient. Thus, a more efficient promoter for gold must be found to improve the selectivity

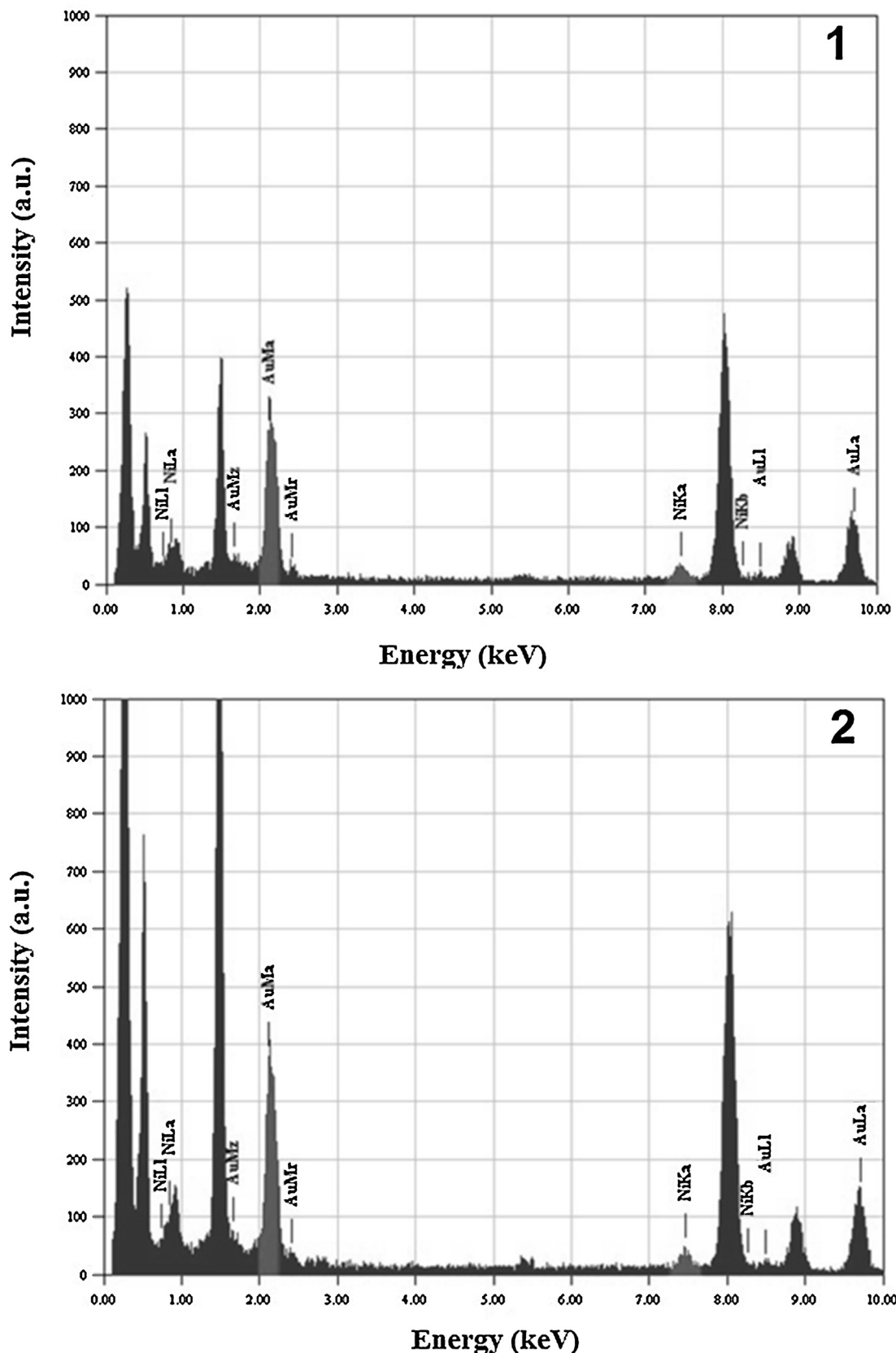


Fig. 6. EDX spectrum of squares 1 and 2 on the HRTEM image of the Au-Ni/Al₂O₃ catalyst. These squares contain both gold and nickel particles.

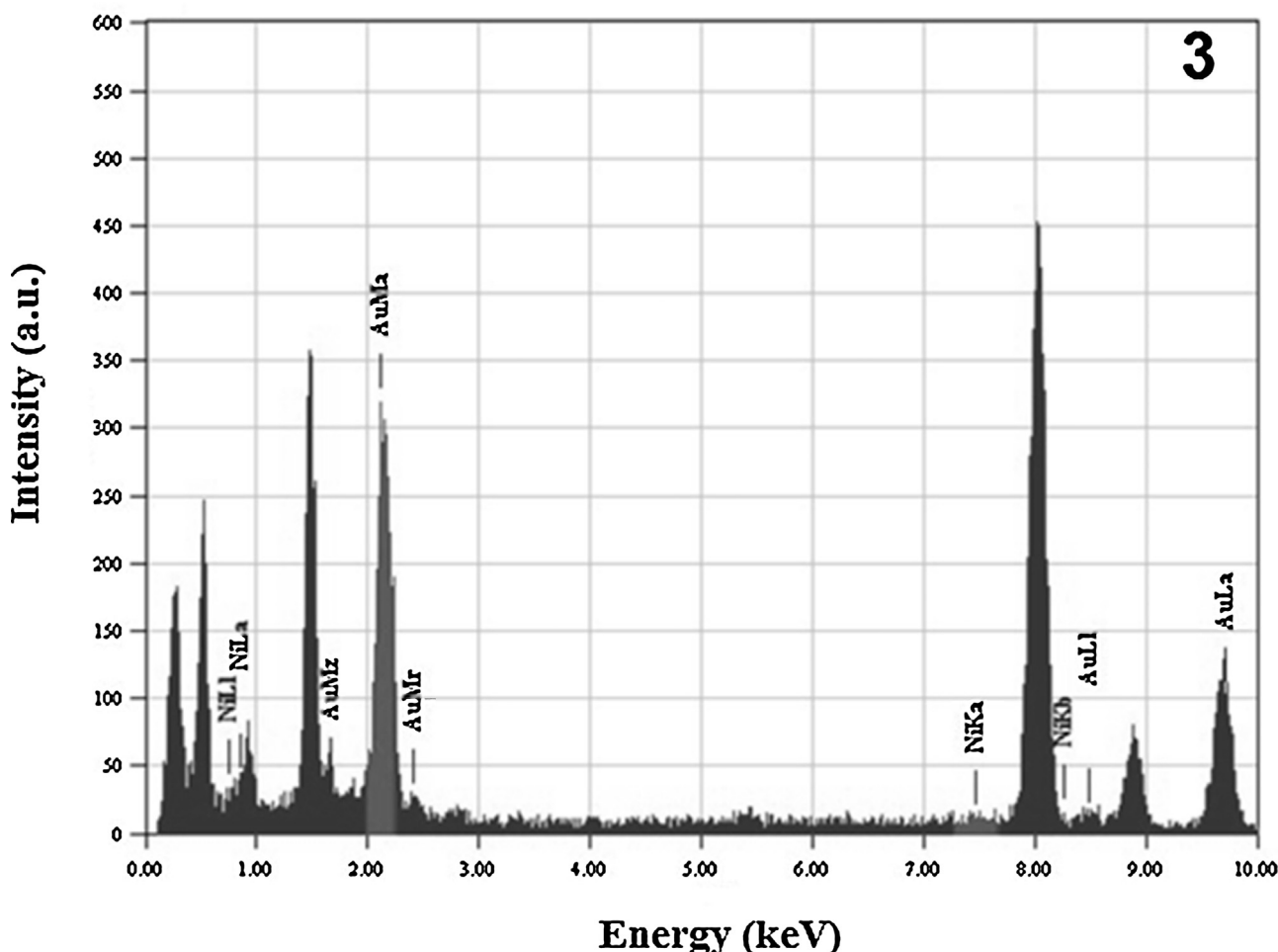


Fig. 7. EDX spectrum of square 3 on the HRTEM image of the Au-Ni/Al₂O₃ catalyst. This square contains primarily gold particles.

of cross-condensation product formation near that produced via homogeneous catalysis.

4. Conclusions

This study shows that the Au/Al₂O₃ and Au-Ni/Al₂O₃ catalysts containing 0.2 wt.% of gold and 0.06 wt.% of nickel are efficient systems for ethanol condensation into 1-butanol and higher linear α -alcohols without using any solvents or alkali compounds. The combined selectivity of C₄, C₆ and C₈ *n*-alcohols exceeded 85% at 63.5% ethanol conversion. For the first time, Au/Al₂O₃ and Au-Ni/Al₂O₃ systems were used for the heterogeneous catalysed cross-condensation of ethanol with isopropanol into pentanol-2. Au-Ni/Al₂O₃ produced the highest pentanol-2 selectivity of 35–37% at 275 °C. The combined selectivity of cross-condensation products (i.e., alcohols and ketones) was found to be 63%–67%. The primary peculiarities of the reaction were also investigated, and it was found that the interaction of gold and nickel oxide particles in a bimetallic system produced a significant increase in the selectivity of cross-condensation products, such as pentanol-2, pentanone-2, heptanone-4 and heptanol-4. This phenomenon may be explained by two phenomena: the structural factor that affects the formation of elongated clusters of Au_n-NiO_{xn}-Au_n-NiO_{xn}, which could coordinate ethanol and isopropanol on a short distance; and the formation of gold cations Auⁿ⁺ (where 1 ≤ n ≤ 3), which likely encourages substrate molecule activation

via dehydrogenation and hydrogen redistribution during catalysis.

Acknowledgments

This study was financially supported by Russian Scientific Foundation Grant No. 15-13-30034 and used the equipment of M.V. Lomonosov Moscow State University (Program of MSU Development).

References

- [1] A. Demirbas, *Biofuels Securing the Planet's Future Energy Needs*, Springer-Verlag, London, 2009.
- [2] Y. Soma, K. Inokuma, T. Tanaka, C. Ogino, A. Kondo, M. Okamoto, T. Hanai, *J. Biosci Bioeng.* 114 (2012) 80–85.
- [3] J. Lee, Y.S. Jang, S.J. Choi, J.A. Im, H. Song, J.H. Cho, D.Y. Seung, E.T. Papoutsakis, G.N. Bennett, S.Y. Lee, *Appl. Environ. Microbiol.* 78 (2012) 1416–1423.
- [4] M. Guerbet, *Comptes Rendus* 128 (1899) 511–513.
- [5] J.T. Kozlowski, R.J. Davis, *ACS Catal.* 3 (2013) 1588–1600.
- [6] X. Chang, L.W. Chuan, L. Yongxin, S.A. Pullarkat, *Tetrahedron Lett.* 53 (2012) 1450–1455.
- [7] D. Gabriels, W.Y. Hernández, B. Sels, P. Van Der Voort, A. Verberckmoes, *Catal. Sci. Technol.* 5 (2015) 3876–3902.
- [8] J.F. Jenck, F. Agterberg, M.J. Droescher, *Green Chem.* 6 (2004) 544–556.
- [9] D. Wang, X.-Q. Guo, Ch.-X. Wang, Ya-N. Wang, R. Zhong, X.-H. Zhu, L.-H. Cai, Z.-W. Gao, X.-F. Hou, *Adv. Synth. Catal.* 355 (2013) 1117–1125.
- [10] S. Ogo, A. Onda, Y. Iwasa, K. Hara, A. Fukuoka, K. Yanagisawa, *J. Catal.* 296 (2012) 24–30.

- [11] T. Tsučida, Sh. Sakuma, T. Takeguchi, W. Ueda, *Ind. Eng. Chem. Res.* 45 (2006) 8634–8642.
- [12] T. Riittonen, K. Eranen, P. Maki-Arvela, A. Shchukarev, A.-R. Rautio, K. Kordas, N. Kumar, T. Salmi, J.-P. Mikkola, *Renew. Energ.* 74 (2015) 369–378.
- [13] M.N. Dvornikoff, M.W. Farrar, *J. Org. Chem.* 22 (1957) 540–542.
- [14] T. Riittonen, E. Toukonity, D.K. Madnani, A.-R. Leino, K. Kordas, M. Szabo, A. Sapi, K. Arve, J. Wärnå, J.-P. Mikkola, *Catalysts* 2 (2012) 68–84.
- [15] A.J. O'Lenick Jr., J.I. Nielsen, *Tetrahedron* 23 (1967) 1723–1733.
- [16] S. Veibel, J.I. Nielsen, *Surfactants Deterg. Agents Colloid Sci.* 4 (2001) 311–315.
- [17] F.-C. Duh, D.-S. Lee, Y.-W. Chen, *Mod. Res. Catal.* 2 (2013) 1–8.
- [18] B. White, M. Yin, A. Hall, D. Le, S. Stolbov, T. Rahman, N. Turro, S. O'Brien, *Nano Lett.* 6 (2006) 2095–2098.
- [19] S. Ordóñez, E. Dhaz, M. Leyn, L. Faba, *Catal. Today* 167 (2011) 71–76.
- [20] G. Jiang, S.J. Pickering, E.H. Lester, N.A. Warrior, *Ind. Eng. Chem. Res.* 49 (2010) 4535–4541.
- [21] K. Shimura, K. Kon, S.M.A.H. Siddiki, Ken-ichi Shimizu, *Appl. Catal. A: Gen.* 462–463 (2013) 137–142.
- [22] J.I.D. Cosimo, G. Torres, C.R. Apesteguia, *J. Catal.* 208 (2002) 114–123.
- [23] S.A. El-Molla, *Appl. Catal. A* 298 (2006) 103–108.
- [24] G. Torres, C.R. Apesteguia, J.I.D. Cosimo, *Appl. Catal. A* 317 (2007) 161–170.
- [25] P. Anbarasan, Z.C. Baer, S. Sreekumar, E. Gross, J.B. Binder, H.W. Blanch, D.S. Clark, F.D. Toste, *Nature* 491 (2012) 235–239.
- [26] S. Sreekumar, Z.C. Baer, E. Gross, S. Padmanaban, K. Goulas, G. Gunbas, S. Alayoglu, H.W. Blanch, D.S. Clark, F.D. Toste, *ChemSusChem* 7 (2014) 2445–2448.
- [27] J. Yang, X. Liu, D.-L. Meng, H.-Y. Chen, Z.-H. Zong, T.-T. Feng, K. Sun, *Adv. Synth. Catal.* 354 (2012) 328–334.
- [28] H.W. Cheung, T.Y. Lee, H.Y. Lui, C.H. Yeung, Ch.P. Lau, *Adv. Synth. Catal.* 350 (2008) 2975–2983.
- [29] M. Haruta, T. Kobayashi, H. Sano, N. Yamada, *Chem. Lett.* 16 (1987) 405–408.
- [30] T. Tabakova, L. Ilieva, I. Ivanov, R. Zanella, J.W. Sobczak, W. Lisowski, Z. Kaszkur, D. Andreeva, *Appl. Catal. B: Environ.* 136–137 (2013) 70–80.
- [31] M.G. Castaño, T.R. Reina, S. Ivanova, M.A. Centeno, J.A. Odriozola, *J. Catal.* 314 (2014) 1–9.
- [32] S.A. Nikolaev, V.V. Smirnov, A. Yu Vasil'kov, V.L. Podshibikhin, *Kinet. Catal.* 51 (2010) 375–379.
- [33] S.A. Nikolaev, N.A. Permyakov, V.V. Smirnov, A. Yu Vasil'kov, S.N. Lanin, 2010, *Kinet. Catal.* 51 (2010) 288–292.
- [34] V.V. Smirnov, S.A. Nikolaev, G.P. Murav'eva, L.A. Tyurina, A. Yu Vasil'kov, 2007, *Kinet. Catal.* 48 (2007) 265–270.
- [35] I.L. Simakova, S. Yu Solkina, B.L. Moroz, O.A. Simakova, S.I. Reshetnikov, I.P. Prosvirin, V.I. Bukhtiyarov, V.N. Parmon, D. Yu Murzin, *Appl. Catal. A* 385 (2010) 136–143.
- [36] S. Gómez-Quero, F. Cárdenas-Lizana, M.A. Keane, *J. Catal.* 303 (2013) 41–49.
- [37] F. Cárdenas-Lizana, D. Lamey, N. Perret, S. Gómez-Quero, L. Kiwi-Minsker, M.A. Keane, *Catal. Commun.* 21 (2012) 46–51.
- [38] H.-L. Jiang, Q. Xu, *J. Mater. Chem.* 21 (2011) 13705–13725.
- [39] A.K. Singh, Q. Xu, *ChemCatChem* 5 (2013) 652–676.
- [40] O.G. Ellert, M.V. Tsodikov, S.A. Nikolaev, V.M. Novotortsev, *Russ. Chem. Rev.* 83 (2014) 718–732.
- [41] T. Takei, T. Akita, I. Nakamura, T. Fujitani, M. Okumura, K. Okazaki, J. Huang, T. Ishida, M. Haruta, *Adv. Catal.* 55 (2012) 1–126.
- [42] M.A. Centeno, K. Hadjiiivanov, Tz. Venkov, Hr. Klimev, J.A. Odriozola, J. Mol. Catal. A: Chem. 252 (2006) 142–149.
- [43] A.N. Pestyakov, V.V. Lunin, N. Bogdanchikova, O.N. Temkin, E. Smolentsev, *Fuel* 110 (2013) 48–53.
- [44] N. Weiher, E. Bus, L. Delannoy, C. Louis, D.E. Ramaker, J.T. Miller, J.A. van Bokhoven, *J. Catal.* 240 (2006) 100–107.
- [45] M. Chen, D.W. Goodman, *Chem. Soc. Rev.* 37 (2008) 1860–1870.
- [46] F. Besenbacher, I. Chorkendorff, B.S. Clausen, B. Hammer, A.M. Molenbroek, J.K. Nørskov, I. Stensgaard, *Science* 279 (1998) 1913.
- [47] O.P. Tkachenko, L.M. Kustov, S.A. Nikolaev, V.V. Smirnov, K.V. Clementiev, A.V. Naumkin, I.O. Volkov, A.Yu. Vasil'kov, D.Yu. Murzin, *Top. Catal.* 52 (2009) 344.
- [48] S.A. Nikolaev, V.V. Smirnov, *Catal. Today* 147 (2009) 336–341.
- [49] M.A. Keane, S. Gómez-Quero, F. Cárdenas-Lizana, W. Shen, *ChemCatChem* 1 (2009) 270–278.
- [50] S.A. Nikolaev, A.V. Chistyakov, M.V. Chudakova, V.V. Kriventsov, E.P. Yakimchuk, M.V. Tsodikov, *J. Catal.* 297 (2013) 296–305.
- [51] S.A. Nikolaev, E.V. Golubina, I.N. Krotova, M.I. Shilina, A.V. Chistyakov, V.V. Kriventsov, *Appl. Catal. B: Environ.* 168–169 (2015) 303–312.
- [52] V.V. Smirnov, S.N. Lanin, A.Yu. Vasil'kov, S.A. Nikolaev, G.P. Murav'eva, L.A. Tyurina, E.V. Vlasenko, *Russ. Chem. Bull.* 54 (2005) 2286–2289.
- [53] A. Wang, X.Y. Liu, C.-Y. Mou, T. Zhang, *J. Catal.* 308 (2013) 258–271.